

Trap-assisted tunneling resistance switching effect in $\text{CeO}_2/\text{La}_{0.7}(\text{Sr}_{0.1}\text{Ca}_{0.9})_{0.3}\text{MnO}_3$ heterostructure

X. G. Chen,¹ J. B. Fu,¹ S. Q. Liu,¹ Y. B. Yang,¹ C. S. Wang,¹ H. L. Du,¹ G. C. Xiong,¹ G. J. Lian,¹ and J. B. Yang^{1,2,a)}

¹School of Physics, Peking University, Beijing 100871, People's Republic of China

²State Key Laboratory for Mesoscopic Physics, School of Physics, Peking University, Beijing 100871, People's Republic of China

(Received 24 May 2012; accepted 4 October 2012; published online 11 October 2012)

We reported the resistance switching (RS) behavior in the epitaxially grown $\text{CeO}_2/\text{La}_{0.7}(\text{Sr}_{0.1}\text{Ca}_{0.9})_{0.3}\text{MnO}_3$ ($\text{CeO}_2/\text{LSCMO}$) heterojunctions on SrTiO_3 substrate. The $\text{CeO}_2/\text{LSCMO}$ device displayed improved switching characteristics as compared to that of metal/manganite device. The switching threshold voltage showed a strong dependence on the thickness of the CeO_2 layer, where a minimum/maximum thickness was required for the appearance of the resistance switching. Both set and reset threshold voltages increase with the increase of the CeO_2 layer thickness due to the trap-assisted electron tunneling effect. In the meantime, the defects or vacancies in the CeO_2 films, in particular, the concentration of the defects or vacancies in the interface between CeO_2 and LSCMO, have a significant impact on the switching effect. These results suggest that the electron tunneling accompanied by a trapping/detrapping process at the interface is likely responsible for the RS effect in the insulator/manganite system. © 2012 American Institute of Physics. [<http://dx.doi.org/10.1063/1.4760221>]

Recently, the resistance switching (RS) effect in the transition metal oxides has attracted much attention due to its potential applications in the next generation of nonvolatile memory.^{1,2} The RS effect was found in various kinds of oxide systems, including binary oxides such as ZrO_2 , TiO_2 , NiO , Fe_2O_3 , and ZnO ; perovskite-type oxides such as SrTiO_3 (STO), Nb-doped STO, and manganite.^{3–13} As for the manganite system, most of the previous studies have been focused on the heterostructures made of a metal and manganite layers.^{14–26} Several resistance switching models were proposed, including conducting filaments due to electric field-induced oxygen vacancy migration,¹⁴ reversible ion migration from electrode,²¹ trapping of carriers, and Mott transition induced by carriers doping at the interface.^{16,17}

The formation of metal oxide interface layer between the metal electrode and manganite was found to be important for the switching effect.^{15,19,22–25} In certain metal-manganite contacts, oxygen may deplete from the manganite surface to form an oxidized metal layer, which becomes an intrinsic insulating barrier between the metal and manganite. However, studies on the properties of the oxide insulator and their contributions to the RS effect are rather limited.¹¹ Thus, we chose CeO_2 as an insulating layer to the epitaxially grown $\text{CeO}_2/\text{La}_{0.7}(\text{Sr}_{0.1}\text{Ca}_{0.9})_{0.3}\text{MnO}_3$ ($\text{CeO}_2/\text{LSCMO}$) junction on SrTiO_3 substrate. The effects of the thickness and defect/vacancies of the insulating layer on the RS behavior were investigated. The RS effect was found to be profoundly influenced by the thickness of the insulating CeO_2 layer and the deposition pressure. Moreover, the RS ratio of R_H/R_L , where R_H and R_L are resistance of high- and low-resistance states,

respectively, are enhanced in the metal/insulator/manganite system when compared to that of metal/manganite system.

Typical $\text{CeO}_2/\text{LSCMO}$ structure was prepared using a pulsed laser deposition technique. A KrF excimer laser ($\lambda = 248 \text{ nm}$) with an energy of 312 mJ and a repetition rate of 6 Hz was used. The LSCMO films with thicknesses of 10 and 100 nm were first deposited on (001)-oriented STO single crystal under an oxygen pressure of 30 Pa, with substrate temperatures of 200 °C and 600 °C, respectively. The CeO_2 films with thickness between 5 and 50 nm were then grown at 600 °C under various O_2 pressures. The electrodes of Ag with the area of less than 1 mm² were paint onto the $\text{CeO}_2/\text{LSCMO}$ junction. The schematic display of the measurement of the two-terminal device is depicted in Fig. 1(a). All the electric measurements were conducted using Keithley 2400 system. A forward voltage bias exerted on the $\text{CeO}_2/\text{LSCMO}$ junction is defined as the current flowing from the Ag electrode on CeO_2 film to LSCMO thin film. The dc voltage was

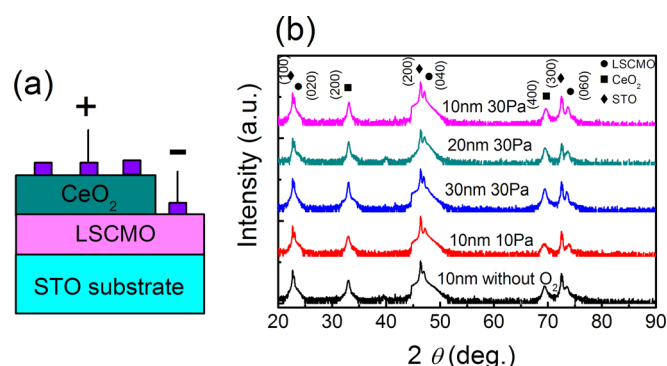


FIG. 1. (a) Sample configuration and measurements of the two-terminal device for $\text{CeO}_2/\text{LSCMO}$ junction. (b) The XRD patterns of $\text{CeO}_2/\text{LSCMO}$ junction with various thicknesses of CeO_2 films (10, 20, and 30 nm) and with various O_2 pressures during deposition (30, 10 Pa, and without O_2).

^{a)} Author to whom correspondence should be addressed. Electronic mail: jbyang@pku.edu.cn.

swept as $0 \rightarrow +V_{\max} \rightarrow 0 \rightarrow -V_{\max}$, and then back to 0 V in the end.

The crystal structure of the films was characterized by x-ray diffraction (XRD) with Cu-K α radiation for θ - 2θ scans (Philips MRD X'pert, wavelength $\lambda = 1.5481 \text{ \AA}$). The θ - 2θ patterns were collected with (010) peak for LSCMO films, and (001) peak for CeO₂ films, indicating that LSCMO and CeO₂ films were epitaxially grown on (001)-oriented STO (Fig. 1(b)). The calculated out-of-plane lattice constants were 7.751 \AA and 5.428 \AA for LSCMO and CeO₂ films, respectively. Compared to the value of 5.410 \AA for the bulk CeO₂, the slightly larger out-of-plane lattice parameter of the CeO₂ film demonstrates that the latter is tensely strained on LSCMO film. This strain is likely resulted from the large lattice mismatch between CeO₂ and LSCMO.²⁷ Moreover, the peaks of CeO₂ films shift slightly to the lower angle with the increase of the film thickness, which corresponds to the release of the strain in the CeO₂ films.

In order to investigate the impacts of the insulating layer on the switching effect, the Ag/CeO₂/LSCMO/Ag systems with various thicknesses of CeO₂ films were prepared. The Ag/LSCMO/Ag system without CeO₂ was also prepared as a control. The I - V curve of the control material shows linear characteristics suggesting that the contact between Ag electrode and the LSCMO film is ohmic (data not shown). No switching effect could be found with different voltage biases. With a CeO₂ layer thicker than 5 nm, however, the rectification behavior is observed in I - V curves (see Fig. 2(a)), indicating the formation of a Schottky-like barrier (potential barrier) at the CeO₂/LSCMO interface. The RS phenomena were clearly shown in the CeO₂/LSCMO system with the thickness of CeO₂ layer of 10–40 nm. When CeO₂ layer

reaches 50 nm in thickness, the switching effect is dramatically degraded. In addition, when a forward voltage bias was applied to the CeO₂ (10 nm)/LSCMO junction, the current abruptly jumps at a threshold voltage of +3 V. Correspondingly, the resistance changes from $\sim 2.0 \times 10^7 \Omega$ to $\sim 2.8 \times 10^4 \Omega$ (RS ratio of $\sim 10^3$). A switch of the device from a high resistance state (HRS) to a low resistance state (LRS) was indicated. This implies that applying voltage to the sample can modify the Schottky-like barrier. The charge carriers are then pulled out of the depleted trapping layer and tunnel through the CeO₂ layer.²⁸ The LRS is kept until a higher reversing voltage switches it back to HRS. When the reversing voltage reaches a threshold of -2.4 V , the resistance of the system increases sharply, corresponding to the switch-back effect from LRS to HRS. The HRS status was then maintained until the next forward set voltage switches it to LRS. Compared to the RS ratio in the metal/manganite system, the one in the insulating-oxide/manganite/STO system is greatly enhanced.

Along with the increase of the thickness of CeO₂ films, the resistance of CeO₂/LSCMO junction increases and the RS ratio decreases (Fig. 2(b)). This indicates that the electrons are more difficult to tunnel through the thicker CeO₂ barrier. Accordingly, both set and reset voltages rise with the increase of CeO₂ thickness (Fig. 2(c)). For the thinner CeO₂ (5 nm)/LSCMO junction, the I - V curve displays Ohmic-like characteristics without hysteresis owing to the high conductivity. Thus, the switching effect is only observed with an appropriate thickness of CeO₂ layer.

In order to investigate the composition effect of the interface layer on the RS ratio, the device with 10 nm CeO₂ insulator layer was prepared under different O₂ pressures. Fig. 3 plots the typical I - V characteristics (under semilog scale) of Ag/CeO₂/LSCMO/Ag devices prepared without O₂, and with O₂ gas pressures of 10 and 30 Pa. As shown in the figure, with a decrease of O₂ pressure during the deposition

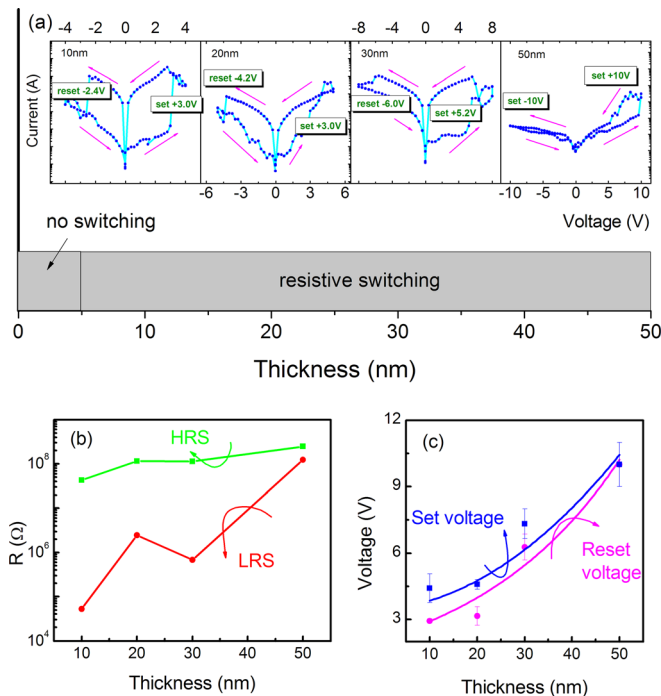


FIG. 2. (a) Thickness dependence of the I - V characteristics for 10, 20, 30, and 50 nm CeO₂ films in CeO₂/LSCMO junction (under semilog scale). (b) The thickness dependence of the RS ratio for the CeO₂/LSCMO junction. (c) The set and reset voltages plotted as a function of CeO₂ thickness in CeO₂/LSCMO system.

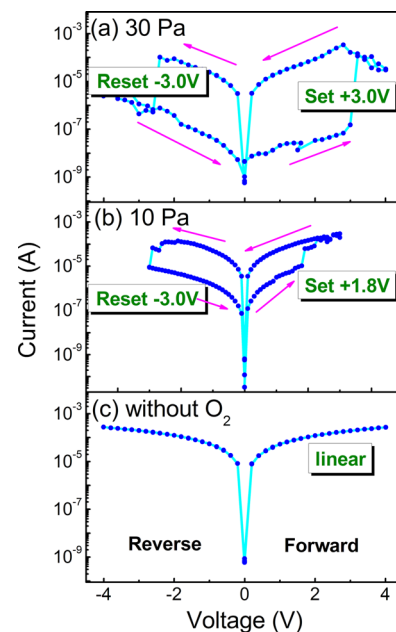


FIG. 3. The I - V characteristics of CeO₂ deposited at various O₂ pressures in CeO₂ (10 nm)/LSCMO system (under semilog scale) (a) 30 Pa, (b) 10 Pa, and (c) without O₂.

of CeO₂ films, the RS ratio is reduced one order of the magnitude; the set voltage changes from +3.0 V (30 Pa O₂) to +1.8 V (10 Pa O₂), and the resistance of CeO₂/LSCMO junction is also reduced [Figs. 3(a) and 3(b)]. Ultimately, the *I-V* curve becomes linear with the CeO₂ film deposited in the absence of O₂ [Fig. 3(c)]. Such a low oxygen pressure during preparation may lead to the loss of oxygen in the CeO₂ film and the formation of oxygen vacancy (*V_o*) in the crystal structure. The interface layer is thus altered and subsequently affecting the band structure, i.e., trapping/detrapping process. Since *V_o* is an n-type doping for CeO₂, the carrier concentration in the system can be greatly enhanced.^{10,26} The carrier density in turn affects the trapping sites/centers in the interface of CeO₂ and LSCMO films. Moreover, the insulating CeO₂ layer becomes conductive in the lower O₂ pressure owing to the enhanced electronic conductivity.¹⁶ The lowered barrier height ϕ_B and built-in potential ϕ_i result in an Ohmic-like contact between CeO₂ and LSCMO.^{10–12} Accordingly, no differences in the trapping and detrapping states can be obtained, eliminating the RS effect in this sample. It suggests that the appropriate amount of carrier is the key to produce suitable barrier height ϕ_B and built-in potential ϕ_i near the interface and to form Schottky-like junction with enough trapping density between CeO₂ and LSCMO. This eventually leads to a maximum value in the hysteresis in the *I-V* curve and a high RS ratio.^{10,16}

The switching effect with a large RS ratio could be obtained in Ag/CeO₂/LSCMO/Ag device with both CeO₂ and LSCMO films deposited at an O₂ pressure of 30 Pa (Fig. 4(a)). On the contrary, either the CeO₂ or LSCMO films deposited without O₂ showed the Ohmic-like characteristics in the *I-V* curves (Figs. 4(b) and 4(c)), suggesting an Ohmic contact between Ag and LSCMO. As no RS effect could be observed with this Ohmic contact, the formation of the

Schottky-like barrier with an appropriate interface is attributed to the switching effect observed in the CeO₂ (10 nm)/LSCMO system.

The temperature dependence of *I-V* curves for the CeO₂ (20 nm)/LSCMO junction is shown in Fig. 4(d). The inset of Fig. 4(d) displays the temperature dependence of resistance for the LSCMO film that undergoes the ferromagnetic to paramagnetic ordering transition at 230 K. The resistance of LSCMO film is less than 1 k Ω from 100 to 300 K, negligible when compared to the system resistance of $\sim 10^7 \Omega$. Thus, the CeO₂ insulator layer and the CeO₂/LSCMO junction make main contribution to the system resistance. With the decrease of temperature, the *I-V* loop becomes larger and the threshold voltage required for the switching behavior increases. The increase of the resistance of CeO₂ layer may account for these changes. The differences of *I-V* loops under various temperatures possibly originate from the variation of Schottky-like barrier height, built-in potential at the interface between CeO₂ and LSCMO film, and variations of activation energy for electrons at different temperatures.^{10–14}

The results shown above illustrate some properties of the switching effect of Ag/CeO₂/LSCMO/Ag device. First, the anodization or electrochemical redox of the Ag metal electrode cannot explain this effect since it could be observed with an inactive Pt-electrode or under an inert He gas environment (data not shown). Second, the RS effect is not observed in the CeO₂ film directly grown on the STO and conductive Pt substrate, making it unlikely that the bulk CeO₂ itself accounts for the RS effect. Therefore, the switching effect is probably originated from the modification of the Schottky-like barrier at the CeO₂/LSCMO interface with an interface trapping or detrapping assisted tunneling process.^{10,28–30} Fig. 5 shows the model of the RS effect in Ag/CeO₂/LSCMO/Ag system. In this work, the CeO₂ could be divided into two parts: one is good band insulator closed to the top electrode; the other one is oxygen vacancies or defects sufficient conductor closed to the interface. A Schottky-like contact forms at the interface between conductive CeO₂ and LSCMO layers due to their different work functions. The lattice mismatch or variation of deposition conditions results in the generation of a number of defects or oxygen vacancies at the interface between CeO₂ and LSCMO films.^{18,20,26} The appearance of defects or oxygen vacancies at the CeO₂/LSCMO interface may lead to the formation of impurity bands at the Schottky-like depletion layer.^{18,21–25} After the initial sweeping, the electrons are injected and trapped at the impurity bands resulting in HRS.

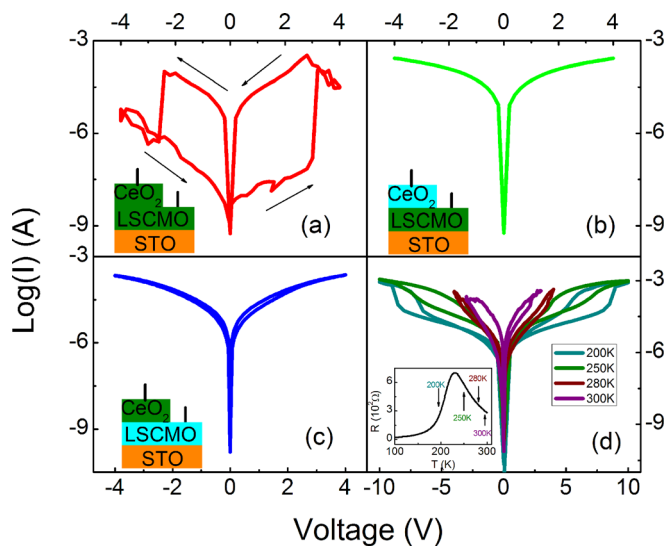


FIG. 4. The *I-V* characteristics of CeO₂ (10 nm)/LSCMO junction deposited at various O₂ pressures (under semilog scale) (a) CeO₂ (30 Pa)/LSCMO (30 Pa), (b) CeO₂ (without O₂)/LSCMO (30 Pa), (c) CeO₂ (30 Pa)/LSCMO (without O₂), (d) temperature dependence of the *I-V* characteristics of CeO₂ (20 nm)/LSCMO system (under semilog scale). The insets (a)–(c) show the corresponding structure of CeO₂ (10 nm)/LSCMO system. The inset (d) shows the temperature dependence of the resistance of LSCMO film measured by the system that analyzes the physical property.

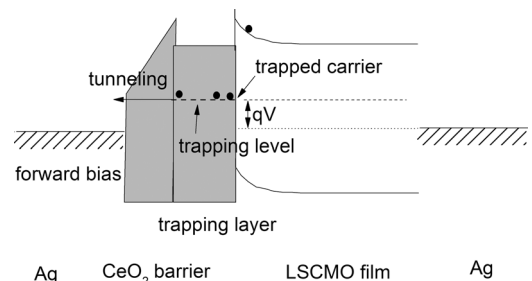


FIG. 5. Schematic band diagram of electronic trapping-assisted tunneling model for the CeO₂/LSCMO system.

Under the specific forward bias, the barrier height ϕ_B and built-in potential ϕ_i at the Schottky-like interface are modified, and the trapped electrons can be pulled out of the impurity band and tunnel through the CeO_2 barrier, leaving the defects or oxygen vacancies at the interface trapping layer. Thus, the system is switched from HRS to LRS, and the LRS is kept until the high reversing reset voltage switches it back to HRS. When reversing the sweeping voltage, the electrons are injected into the impurity band and stored at the interface trapping layer, preventing the electrons hopping at the interface. As a result, the system switches back to HRS. Moreover, under the external electric field, the defects or oxygen vacancies could be moved close to or away from the interface, which leads to decrease or increase in the potential barrier width helping the carrier trapping or detrapping assisted tunneling process. With the increase of the thickness of CeO_2 insulating layer, the energy needed to tunnel through the insulating barrier increases. Thus, the higher set and reset voltages are needed to supply the extra energy to switch the device.

We reported the resistance switching behavior in epitaxially grown $\text{CeO}_2/\text{LSCMO}$ heterostructure. The switching voltage strongly depends on the thickness of the CeO_2 thin film, and a minimum/maximum thickness is required for the resistance switching. The defects or vacancies in the CeO_2 films, in particular, the defects or vacancies between CeO_2 and LSCMO, have a strong impact on the resistance switching effect. Our data suggest that the RS effect in the insulator/magnetite system is largely resulted from the trapping-assisted carrier tunneling at the interface. Under the voltage bias, the electrons tunnel through the CeO_2 barrier and then trapped or detrapped at the impurity band, resulting in the high or low resistance state.

This work was supported by the National Natural Science Foundation of China (Grant Nos. 50971003 and 51171001), the National Basic Research Program of China (No. 2010CB833104, MOST of China), the National High Technology Research and Development Program of China (No. 2011AA03A403), and the program for New Century Excellent Talents (NCET-10-1097).

¹A. Sawa, *Mater. Today* **11**, 28 (2008).

²R. Waser and M. Aono, *Nature Mater.* **6**, 833 (2007).

³S. H. Kim, H. Y. Jeong, S. Y. Choi, and Y. K. Choi, *Appl. Phys. Lett.* **97**, 033508 (2010).

- ⁴D. C. Kim, S. Seo, S. E. Ahn, D. S. Suh, M. J. Lee, B. H. Park, I. K. Yoo, I. G. Baek, H. J. Kim, E. K. Yim, J. E. Lee, S. O. Park, H. S. Kim, U. I. Chung, J. T. Moon, and B. I. Ryu, *Appl. Phys. Lett.* **88**, 202102 (2006).
- ⁵Y. S. Chen, B. Chen, B. Gao, F. F. Zhang, Y. J. Qiu, G. J. Lian, L. F. Liu, X. Y. Liu, R. Q. Han, and J. F. Kang, *Appl. Phys. Lett.* **97**, 262112 (2010).
- ⁶S. Lee, H. Kim, D. J. Yun, S. W. Rhee, and K. Yong, *Appl. Phys. Lett.* **95**, 262113 (2009).
- ⁷X. B. Yan, Y. D. Xia, H. N. Xu, X. Gao, H. T. Li, R. Li, J. Yin, and Z. G. Liu, *Appl. Phys. Lett.* **97**, 112101 (2010).
- ⁸K. Szot, W. Speier, G. Bihlmayer, and R. Waser, *Nature Mater.* **5**, 312 (2006).
- ⁹X. J. Zhu, W. J. Su, Y. W. Liu, B. L. Hu, L. Pan, W. Lu, J. D. Zhang, and R. W. Li, *Adv. Mater.* **24**, 3941 (2012).
- ¹⁰X. G. Chen, X. B. Ma, Y. B. Yang, L. P. Chen, G. C. Xiong, G. J. Lian, Y. C. Yang, and J. B. Yang, *Appl. Phys. Lett.* **98**, 122102 (2011).
- ¹¹R. Muenstermann, T. Menke, R. Dittmann, and R. Waser, *Adv. Mater.* **22**, 4819 (2010).
- ¹²T. Fujii, M. Kawasaki, A. Sawa, Y. Kawazoe, H. Akoh, and Y. Tokura, *Phys. Rev. B* **75**, 165101 (2007).
- ¹³Y. S. Chen, L. P. Chen, G. J. Lian, and G. C. Xiong, *J. Appl. Phys.* **106**, 023708 (2009).
- ¹⁴R. Fors, S. I. Khartsev, and A. M. Grishin, *Phys. Rev. B* **71**, 045305 (2005).
- ¹⁵K. Tsubouchi, I. Ohkubo, H. Kumigashira, M. Oshima, Y. Matsumoto, K. Itaka, T. Ohnishi, M. Lippmaa, and H. Koinuma, *Adv. Mater.* **19**, 1711 (2007).
- ¹⁶Q. Wang, L. D. Chen, X. J. Liu, W. D. Yu, and X. M. Li, *Appl. Phys. A* **96**, 643 (2009).
- ¹⁷D. S. Shang, Q. Wang, L. D. Chen, R. Dong, X. M. Li, and W. Q. Zhang, *Phys. Rev. B* **73**, 245427 (2006).
- ¹⁸Z. Q. Liu, D. P. Leusink, W. M. Lü, X. Wang, X. P. Yang, K. Gopinadhan, Y. T. Lin, A. Annadi, Y. L. Zhao, A. R. Barman, S. Dhar, Y. P. Feng, H. B. Su, G. Xiong, T. Venkatesan, and Ariando, *Phys. Rev. B* **84**, 165106 (2011).
- ¹⁹C. Y. Dong, D. S. Shang, L. Shi, J. R. Sun, B. G. Shen, F. Zhuge, R. W. Li, and W. Chen, *Appl. Phys. Lett.* **98**, 072107 (2011).
- ²⁰J. N. Eckstein, *Nature Mater.* **6**, 473 (2007).
- ²¹A. Baikalov, Y. Q. Wang, B. Shen, B. Lorenz, S. Tsui, Y. Y. Sun, Y. Y. Xue, and C. W. Chu, *Appl. Phys. Lett.* **83**, 957 (2003).
- ²²S. Asanuma, H. Akoh, H. Yamada, and A. Sawa, *Phys. Rev. B* **80**, 235113 (2009).
- ²³A. Sawa, T. Fujii, M. Kawasaki, and Y. Tokura, *Appl. Phys. Lett.* **85**, 4073 (2004).
- ²⁴T. Yamamoto, R. Yasuhara, I. Ohkubo, H. Kumigashira, and M. Oshima, *J. Appl. Phys.* **110**, 053707 (2011).
- ²⁵H. Kaji, H. Kondo, T. Fujii, M. Arita, and Y. Takahashi, *IOP Conf. Ser.: Mater. Sci. Eng.* **8**, 012032 (2010).
- ²⁶A. Kalabukhov, R. Gunnarsson, J. Börjesson, E. Olsson, T. Claesson, and D. Winkler, *Phys. Rev. B* **75**, 121404(R) (2007).
- ²⁷Y. R. Wang, T. Mori, J. G. Li, and T. Ikegami, *J. Am. Ceram. Soc.* **85**, 3105 (2002).
- ²⁸R. Meyer, L. Schloss, J. Brewer, R. Lambertson, W. Kinney, J. Sanchez, and D. Rinerson, in Proceedings of NVMTS (2008), p. 54.
- ²⁹R. Waser, R. Dittman, G. Stainkov, and K. Szot, *Adv. Mater.* **21**, 2632 (2009).
- ³⁰S. M. Yu, X. M. Guan, and H. S. P. Wong, *Appl. Phys. Lett.* **99**, 063507 (2011).